

10K is Enough: An Ultra-Lightweight Binarized Network for Infrared Small-Target Detection

Biqiao Xin^{1*}, Qianchen Mao^{1*}, Bingshu Wang^{1†}, Jiangbin Zheng¹,
Yong Zhao², C.L. Philip Chen³

¹School of Software, Northwestern Polytechnical University,

²Shenzhen Graduate School, Peking University,

³South China University of Technology

Abstract

The widespread deployment of Infrared Small-Target Detection (IRSTD) algorithms on edge devices necessitates the exploration of model compression techniques. Binarized neural networks (BNNs) are distinguished by their exceptional efficiency in model compression. However, the small size of infrared targets introduces stringent precision requirements for the IRSTD task, while the inherent precision loss during binarization presents a significant challenge. To address this, we propose the **Binarized Infrared Small-Target Detection Network (BiisNet)**, which preserves the core operations of binarized convolutions while integrating full-precision features into the network’s information flow. Specifically, we propose the **Dot Binary Convolution**, which retains fine-grained semantic information in feature maps while still leveraging the binarized convolution operations. In addition, we introduce a smooth and adaptive **Dynamic Softsign function**, which provides more comprehensive and progressively finer gradient during backpropagation, enhancing model stability and promoting an optimal weight distribution. Experimental results demonstrate that **BiisNet** not only significantly outperforms other binary architectures but also has strong competitiveness among state-of-the-art full-precision models.

1. Introduction

Infrared Small-Target Detection (IRSTD) requires real-time processing in resource-constrained edge scenarios, such as rescue devices and military equipment deployments, where cloud computing is infeasible due to data privacy concerns or limited network connectivity. However, state-of-the-art (SOTA) deep-learning-based IRSTD algorithms [22, 39, 43] typically require over 40 GFLOPs computa-

*These authors contributed equally to this work.

†Corresponding author.

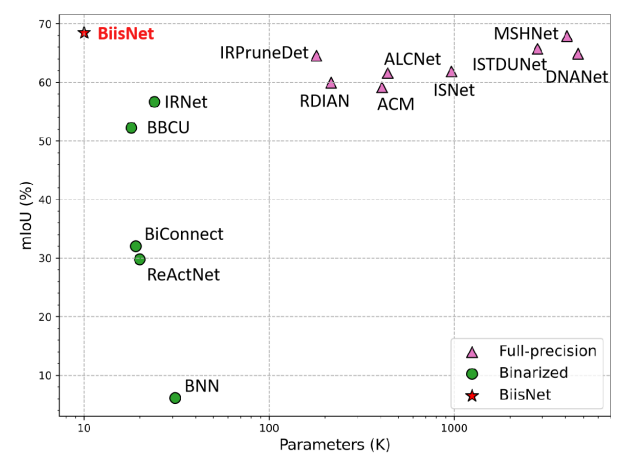


Figure 1. The comparison between the proposed BiisNet with SOTA methods on the IRSTD-1K dataset in terms of the $mIoU$ metric. The green dots represent the binary neural network architectures, the purple triangles indicate the full-precision neural networks, and the red star represents our BiisNet.

tions, far exceeding the capacity of the majority of resource-constrained edge devices [11] (e.g., 9.69GFLOPs on Raspberry Pi-4B (4GB) [28]). Despite rapid advancements in IRSTD methods, their reliance on computational precision and network parameters renders them impractical for resource-constrained edge deployment.

To deploy neural networks in edge scenarios, compression and acceleration techniques are typically required. Recently, a series of techniques have been invested for the deployment of neural network models, for example, model quantization [20], model pruning [10], and knowledge distillation [19]. In this paper, we investigate the optimization effects of model quantization using binary neural networks (BNNs) [17] on IRSTD models. By quantizing both weights and activations to 1-bit, BNNs achieve a remarkable $32\times$ reduction in memory usage and $64\times$

computational efficiency improvement [31]. This makes BNNs particularly well-suited for deployment on resource-constrained CPUs.

However, the extreme compression of data precision from 32-bit floating-point to 1-bit significantly reduces the model’s representational capacity. This drastic reduction leads to a substantial loss in expressiveness compared to full-precision floating points. This limitation becomes problematic for high-precision, dense detection tasks like IRSTD. Directly applying model binarization in such scenarios may pose several challenges: 1) infrared small targets typically occupy only a few pixels, and directly using binary feature representation can easily lead to significant feature degradation or even complete loss of target information; 2) the forward propagation of full-precision information in BNNs is inherently limited by the computational constraints of binary convolution operations, leading to significant accuracy loss; 3) traditional BNNs approximate the non-differentiable sign function using piecewise linear [30] or quadratic [23] functions during backpropagation. Nonetheless, these approximations often result in either substantial errors or increased computational cost, further affecting model performance.

In light of these insights, our motivation is to preserve a high-precision information flow in both forward and backward propagation, thereby alleviating the information loss induced by binarization. We redesign a binary model tailored for IRSTD, namely Binarized Infrared Small-Target Detection Network (BiisNet). BiisNet consists solely of the simplest convolutional operators, enabling efficient inference on edge devices using XNOR (exclusive NOR) operations and BitCount logic operations. To obtain high-precision information flow in forward propagation, we introduce Dot Binary Convolution (DB Conv). It interacts with the full-precision activation using the element-wise multiplication following the core binarized convolution. To get precise gradient during backpropagation, we employ a Dynamic SoftSign Function (DySoftSign) in the Straight-Through Estimator [1] (STE). This function dynamically reduces approximation errors in the gradient calculation of the non-differentiable Sign function, enhancing training stability and accuracy.

As shown in Fig. 1, BiisNet achieves a remarkable advantage in $mIoU$, outperforming the current SOTA BNNs by nearly 12%. More notably, BiisNet surpasses many leading full-precision IRSTD models while maintaining an exceptionally low parameter count and computational cost.

Our contributions are as follows:

- We propose a novel BNN-based algorithm, BiisNet, for IRSTD. To the best of our knowledge, this is the first work addressing the problem of binarized IRSTD.
- We introduce Dot Binary Convolution, which combines full-precision activations with binary convolution outputs

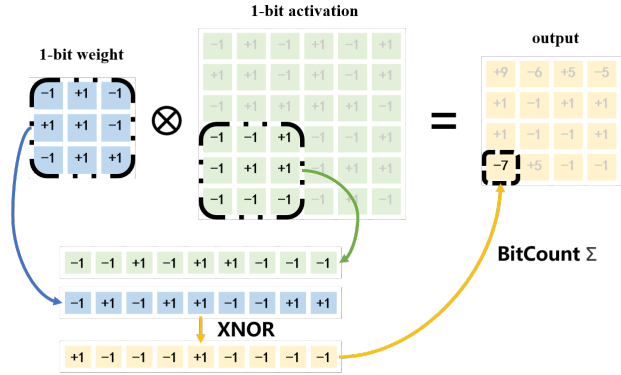


Figure 2. Schematic diagram of the binary convolution process. The weight and activation at 1-bit precision are first calculated through XNOR and the summed up by BitCount.

via element-wise multiplication. This approach enables efficient feature extraction with minimal parameters and reduced computational cost.

- We design Dynamic SoftSign function as an adaptive and smooth approximation of the Sign function during backpropagation. This strategy significantly reduces gradient approximation errors, enhancing the stability of the model training.
- Experiments on multiple benchmarks demonstrate that BiisNet outperforms SOTA BNN architectures by 12% in $mIoU$. Furthermore, it achieves competitive performance against full-precision models with only 10k parameters, which is 0.019% of UIUNet.

2. Preliminaries

In this section, we brief the pipeline of binary convolution and its propagation process, which serve as the foundation for the DB Conv and DySoftSign in BiisNet.

Classical full-precision convolution requires a given input $a \in \mathbb{R}^{c \times h \times w}$ and convolutional weights $w \in \mathbb{R}^{n \times c \times k \times k}$. Through the convolution operation, the output is obtained as $y \in \mathbb{R}^{n \times h' \times w'}$, which can be expressed as:

$$y = a \otimes w. \quad (1)$$

BNN quantizes the convolution operation of CNN to accelerate inference. The sign function $Sign()$ is applied to binarize the input a and the weights w :

$$Sign(a) = \begin{cases} -1, & a < 0 \\ +1, & a \geq 0. \end{cases} \quad (2)$$

As shown in Fig. 2, the core binary convolution operation lies in performing convolution computations on binarized inputs and weights using the bit-wise XNOR operation (denoted as \oplus) and BitCount:

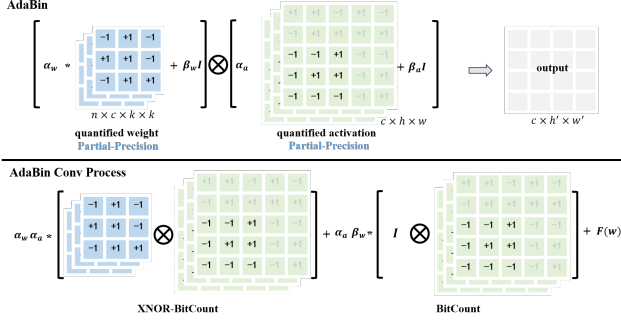


Figure 3. Schematic diagram of the AdaBin [47] computation process. The 1-bit weight and activation are quantified by α_w , β_w and α_a , β_a . Then, associative law is applied to conduct the convolution. The I represents the identity matrix, and $F(w)$ represents the extra computation with w .

$$y = \text{BitCount}(a_b \oplus w_b). \quad (3)$$

The representation of 1-bit feature is weaker than that of full-precision features, directly applying binary convolution to general architectures often leads to a dramatic decline in model performance. Thus, many existing works [17, 21, 36, 47] aim to enhance model expressiveness by introducing some full-precision values without affecting the core binary computation process, as shown in Tab. 1. For example, as shown in Fig. 3, AdaBin [47] assumes that convolution weights typically follow a Bell-shaped Distribution [46]. By minimizing the Kullback-Leibler Divergence (KLD), the weights are re-parameterized as:

$$w_b = \alpha_w b_w + \beta_w, \quad b_w \in \{-1, +1\}, \quad (4)$$

where β_w represents the mean of the weights:

$$\beta_w = E(w) \approx \frac{1}{c \times k \times k} \sum_{m=0}^{c-1} \sum_{j=0}^{k-1} \sum_{i=0}^{k-1} w_{m,j,i}. \quad (5)$$

The scaling factor α_w is defined as:

$$\alpha_w = \frac{\|w - \beta_w\|_2}{\sqrt{c \times k \times k}}, \quad (6)$$

where α_w and β_w are channel-wise parameters.

Similarly, AdaBin also quantizes activation values but employs two learnable parameters, α_a and β_a , for quantization. Although this approach avoids the additional regularization computations introduced in Eqs. (4) to (6), it does not guarantee quantization accuracy when the sample disparity is too large.

Despite this limitation, the quantization framework maintains the efficiency of XNOR and BitCount operations

in binary convolution by exploiting the associative property of these scalar parameters. Meanwhile, introducing a small number of full-precision parameters to quantize and dequantize both weights and activations helps capture the underlying feature distribution, thereby mitigating the accuracy degradation typically associated with binarization.

Since the $\text{Sign}()$ function in Eq. (2) is non-differentiable, the STE method is employed for gradient approximation during backpropagation:

$$\begin{aligned} \text{STE}(X_f) &= \text{Sign}(X_f).detach() \\ &\quad - f_{\text{Appr}}(X_f).detach() \\ &\quad + f_{\text{Appr}}(X_f), \end{aligned} \quad (7)$$

where $f_{\text{Appr}}(X_f)$ represents a differentiable function that approximates the Sign function, and $.detach()$ represents the gradient truncation mechanism.

The backpropagation then processes the gradient of $f_{\text{Appr}}(X_f)$:

$$\text{STE}'(X_f) = f'_{\text{Appr}}(X_f). \quad (8)$$

Some earlier approaches to defining f_{Appr} include functions such as $\text{Clip}(x)$ [30], $\text{Quad}(x)$ [23], and scalable hyperbolic tangent function $\text{Tanh}(x)$ [2].

However, these functions present significant issues. First, the approximation error is relatively large compared to $\text{Sign}()$. Second, when the activation function exceeds the range of $[-1, 1]$, the gradient becomes zero, preventing the update of model weights. Finally, the reliance of $\text{Tanh}(x)$ on transcendental function operations increases computational complexity.

3. The Proposed BiisNet

3.1. Overall Architecture

Current CNN [3, 7, 37] and Transformer-based[35, 38, 44] models typically involve a substantial number of parameters and high computational costs. They typically incorporate complex operations, such as self-attention, which are difficult to implement on resource-constrained edge devices. To address this challenge, we propose BiisNet, which is optimized for the ease of deployment while maintaining good performance.

Inspired by the successful applications of U-shaped [32] architectures such as ACM [7], ISNet [43], and SpirDet [26] in the field of IRSTD, the proposed BiisNet is designed with a streamlined U-shaped semantic segmentation architecture, as shown in Fig. 4(a).

3.2. The Binary Block

As the basic building block of the encoder, bottleneck and decoder, the Binary Block consists of three main components: a Binary Convolution Layer, a ReDistribution Mod-

$w \setminus a$	-1	$+1$	$w \setminus a$	0	$+1$	$w \setminus a$	-1	$+1$	$w \setminus a$	a_{b1}	a_{b2}	$w \setminus a$	a_{full}
-1	$+1$	-1	-1	0	-1	0	0	0	w_{b1}	$a_{b1}w_{b1}$	$a_{b2}w_{b1}$	w_{b1}	$a_{full}w_{b1}$
$+1$	-1	$+1$	$+1$	0	$+1$	$+1$	-1	$+1$	w_{b2}	$a_{b1}w_{b2}$	$a_{b2}w_{b2}$	w_{b2}	$a_{full}w_{b2}$
	(a) BNN [17]			(b) SiBNN [36]			(c) SiMaN [21]			(d) AdaBin [47]			(e) DBConv (Ours)

Table 1. Feature representation comparison of binarization methods. a denotes the binarized input activation, w represents the binarized weight parameters, with $a_{b1}, a_{b2}, w_{b1}, w_{b2} \in \mathbb{R}$ as quantified values, and $a_{full} \in \mathbb{R}$ denoting full-precision activation.

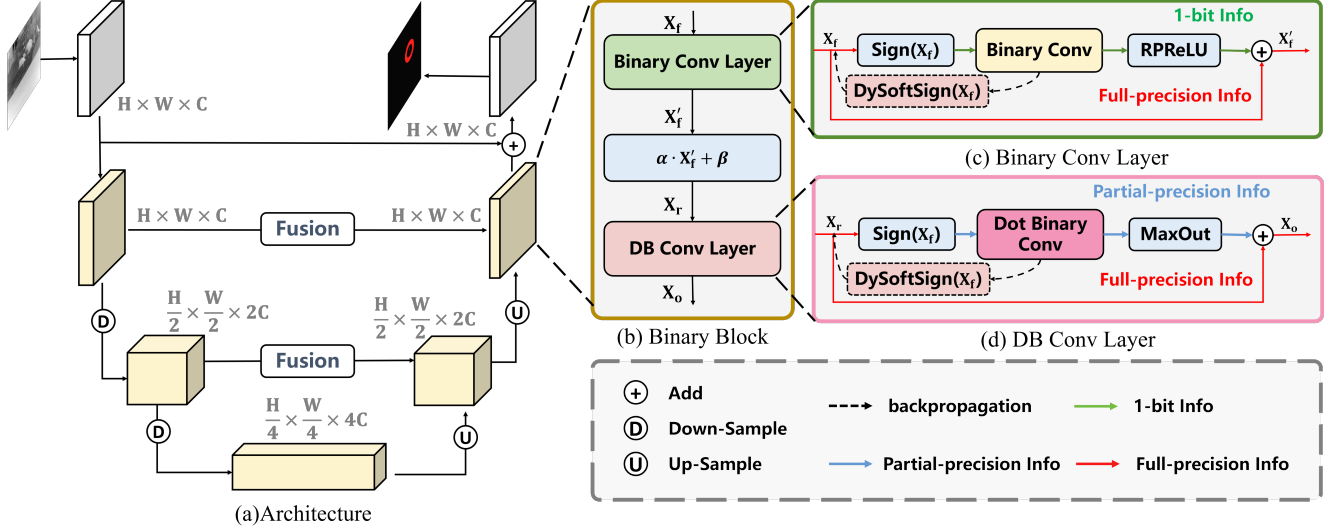


Figure 4. The overall architecture of BiisNet. (a) the U-shaped network architecture with hierarchical feature fusion. (b) the Binary Block, which consists of a Binary Convolution Layer, a ReDistribution layer, and a Dot Binary Convolution (DB Conv) Layer. (c) the Binary Convolution Layer, which preserves 1-bit information in the main branch via binary convolution. (d) the DB Conv Layer, which utilizes Dot Binary Convolution and MaxOut to preserve partial-precision activations.

ule, and a DB Conv Layer. The input feature map \mathbf{X}_f is processed through these stages to produce the output \mathbf{X}_o .

The Binary Convolution Layer operates as:

$$\mathbf{X}'_f = \text{RPRReLU}(f_{BCConv}(\text{Sign}(\mathbf{X}_f))) + \mathbf{X}_f. \quad (9)$$

After completing the binarization operation, the input undergoes binary convolution using XNOR and BitCount operations, following a channel-wise non-linear activation called RPRReLU.

$$\text{RPRReLU}(y_i) = \begin{cases} y_i - a_i + b_i, & y_i > a_i \\ c_i \cdot (y_i - a_i) + b_i, & y_i \leq a_i, \end{cases} \quad (10)$$

where $y_i \in \mathbb{R}$ is the value of the i -th channel in the input Y , and a_i, b_i, c_i are learnable parameters. Subsequently, the activation obtained from RPRReLU will be summed with the precision-preserved input using a residual connection.

The ReDistribution Module refines the feature representation, given by:

$$\mathbf{X}_r = \alpha \cdot \mathbf{X}'_f + \beta. \quad (11)$$

The DB Conv Layer operates as:

$$\mathbf{X}_o = \text{MaxOut}(f_{DBConv}(\text{Sign}(\mathbf{X}_r))) + \mathbf{X}_r. \quad (12)$$

The DB Conv f_{DBConv} fully preserves the full-precision information of the input X_r , while the activation function adopts the Maxout function to strengthen the non-linearity of the feature representation. A detailed explanation of f_{DBConv} will be provided in the Sec. 3.3.

As shown in Fig. 4(b)–(d), a central feature of the Binary Block is the precision information flow. A common practice to preserve full-precision information is to employ residual connections (indicated by the red arrow) to enable incremental refinement of feature maps. However, it is insufficient since the residual branch merely forwards unprocessed information without learnable transformations. In the main branch of Binary Conv Layer, although the 3×3 binary convolution (indicated by the green arrow) effectively

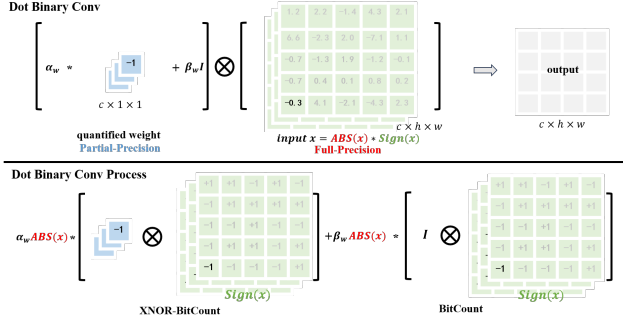


Figure 5. The schematic diagram of the proposed Dot Binary Convolution. The 1-bit weight is quantified by α_w and β_w into partial-precision. It is then computed with the full-precision activation by the associative law.

captures spatial cues, it retains only 1-bit precision and thus produces low-fidelity outputs. In the DB Conv layer (indicated by the blue arrow), the convolution result is combined with full-precision features via element-wise multiplication, preserving fine-grained information flow. This design enables BiisNet to achieve a partial-precision information flow that closely approximates full-precision networks, which is especially vital in IRSTD.

3.3. The Dot Binary Convolution

To address the challenges of precision loss of binarization, we introduce the Dot Binary Convolution (DB Conv). DB Conv extends the property of Adabin in Sec. 2 by utilizing non-trainable α_w and β_w to quantize convolution weights during the convolution process. Instead of employing learnable parameters α_a and β_a to fit the activation distribution, which fail to accurately match the actual sample distribution, DB Conv directly employs full-precision activation values. This approach allows DB Conv to achieve computation accuracy close to that of conventional convolution while maintaining the minimal parameter count and ultra-low computational cost.

As shown in Fig. 5, Dot Binary Convolution is essentially a 1×1 depth-wise convolution, with the weight W as a combination of the binary core weight W_b and the scaling factors α_w and β_w .

$$W = \alpha_w W_b + \beta_w. \quad (13)$$

The parameter β_w is defined as:

$$\beta_w = E(w) \approx \frac{1}{c} \sum_{m=0}^{c-1} w_m. \quad (14)$$

The scaling factor α_w is computed as:

$$\alpha_w = \|w - \beta_w\|_2 = \sqrt{\sum_{m=1}^C (w_m - \beta_w)^2}. \quad (15)$$

The activation value a is decomposed into the product of its absolute value $ABS(a)$ and sign $Sign(a)$.

$$a = ABS(a) * Sign(a), \quad (16)$$

where $*$ denotes the element-wise multiplication.

As a result, the convolution satisfies both the associative and distributive properties of multiplication, allowing the binary components to still be efficiently computed using XNOR and BitCount operations.

$$\begin{aligned} Y &= a \otimes W \\ &= (ABS(a) * Sign(a)) \otimes (\alpha_w W_b + \beta_w) \\ &= \alpha_w ABS(a) * (Sign(a) \otimes W_b) + \beta_w a \\ &= \alpha_w ABS(a) * Y_b + \beta_w a, \end{aligned} \quad (17)$$

where the Y_b is the convolution result computed efficiently via XNOR \oplus and BitCount.

$$Y_b = \text{BitCount}(\text{Sign}(a) \oplus W_b). \quad (18)$$

Furthermore, since α_w and β_w are non-trainable scalars, they allow for highly efficient computation on feature map tensors. The entire computation pipeline remains optimized for XNOR-based binary operations, with only lightweight channel-wise multiplications required to integrate the scaling and bias factors.

Compared to AdaBin convolution unit, DB Conv contains much less parameters. The AdaBin convolution has the parameter count of:

$$64 \times c + n \times c \times k \times k, \quad (19)$$

where the 64 additional parameters correspond to the two floating-point scaling factors (α_w and β_w), while n represents the number of output channels, and $c \times k \times k$ denotes the size of the binarized convolution kernel. In contrast, the depth-wise DB Conv only has $64 + c$ parameters. For example, assuming $n = c = 64$, our DB Conv reduces the parameter count by approximately 320 times.

In summary, DB Conv achieves a substantial reduction in network parameters while maintaining high computational efficiency through minimal additional computation. By preserving full-precision activation values in the form of $ABS(a)$, DB Conv ensures that critical semantic information from the feature maps is retained, effectively mitigating the information loss typically associated with binary networks. This refined feature representation, combined with the computational efficiency of XNOR-based operations, bridges the performance gap between BNNs and

full-precision models in IRSTD while maintaining ultra-low model size.

3.4. The Dynamic SoftSign

To efficiently update the gradient information during back-propagation, we introduce a simple and effective method, namely Dynamic SoftSign (DySoftSign), defined as follows:

$$f_{Appr}(x) = DySoftSign(x) = \frac{kx}{1 + |kx|}, \quad (20)$$

where $k \in \mathbb{R}^+$ is a learnable parameter initialized to a small value of 0.001.

The derivative of $DySoftSign(x)$ is given by:

$$DySoftSign'(x) = \frac{d}{dx} DySoftSign(x) = \frac{k}{(1 + |kx|)^2}. \quad (21)$$

Notably, this function involves only basic addition, absolute value, and division operations, making it computationally more efficient compared to the extended $Tanh(x)$. Moreover, since $DySoftSign(x)$ exhibits a smoother gradient variation than $Tanh(x)$, it enhances model stability and accelerates convergence during training.

Theoretically, the approximation error of the $DySoftSign(x)$ is inversely proportional to k , given by Eq. (22).

$$Err(k) = \frac{2}{k} \int_1^{+\infty} \frac{1}{(1+t)^2} dt = \frac{2}{k}. \quad (22)$$

This demonstrates that the error can be adaptively minimized within a neural network. During early training stages, a smaller k allows $DySoftSign$ to provide a smoother activation function over a wider input range, facilitating faster weight updates and mitigating the dead zone issue. As training progresses, increasing k enables the model to approximate $Sign()$ more closely. The proof of Eq. (22) can be found in the Supplementary Material.

4. Experiments

In this section, we demonstrate the effectiveness and superiority of the proposed BiisNet by comparing it with SOTA BNNs and full-precision IRSTD methods. In addition, we conduct ablation studies to systematically analyze the architectural improvements of BiisNet. The comparative experiments are performed on the SIRST [7], NUDT-SIRST [18] and IRSTD-1K [43] datasets.

4.1. Evaluation Metrics

To evaluate the detection performance of the proposed approach, we employ Probability of Detection (Pd), False

Alarm Rate (Fa), and mean Intersection over Union ($mIoU$) as key metrics. Following prior works, we use binary operations per second (OPs) as an indicator of the computational complexity of the binary components, which is computed as $OPs^b = OPs^f/64$, $OPs^f = \text{FLOPs}$. For the parameter count ($Params$) of the binary components, we compute $Params_b = Params_f/32$. Here, the superscripts b and f denote the binary and full-precision components, respectively. The total computational cost and parameter count of the model are then given by $OPs = OPs^b + OPs^f$, $Params = Params_b + Params_f$. All OPs values in our experiments are computed using a modified version of the torch_flops open-source tool [25].

4.2. Experimental Setup

We implement BiisNet using PyTorch and train it for 400 epochs on a single NVIDIA GeForce RTX 3090 using the AdamW optimizer with a cosine annealing learning rate scheduler. The SoftIoU loss is selected in the experiment.

4.3. Quantitative Analysis

To demonstrate the effectiveness of our method, BiisNet is compared with SOTA methods across different categories, including various model-based full-precision approaches such as Top-Hat [34], Max-Median [8], RLCM [12], WSLCM [15], TLLCM [13], MSLCM [27], MSPCM [27], IPI [9], NRAM [42], RIPT [5], PSTNN [41], and MSLSTIPT [14], multiple 1-bit BNN-based methods including BiConnect [4], BNN [17], Bi-realNet [23], IRNet [29], ReActNet [24], and BBCU [40], and various deep-learning-based full-precision methods such as ACM [7], ALCNet [6], ISNet [43], RDIAN [33], DNANet [18], IST-DUNet [16], UIUNet [39], IRPruneDet [45], and MSHNet [22].

As shown in Sec. 3.4, experimental results on the IRSTD-1K dataset indicate that directly applying SOTA BNN-based methods to IRSTD leads to unsatisfactory performance. The proposed BiisNet, with only 10K parameters and a computational cost of 0.35 GFLOPs, achieves significantly superior performance over all SOTA binary networks. Specifically, BiisNet outperforms BNN, BiConnect, Bi-realNet, IRNet, ReActNet, and BBCU in terms of $mIoU$, Pd , and Fa , achieving $mIoU$ improvements of 62.35%, 36.41%, 12.69%, 38.69%, 11.78%, and 16.22%, respectively. This suggests that BiisNet effectively preserves high-precision information flow, mitigating accuracy degradation, which is particularly crucial in precision-sensitive IRSTD tasks.

Furthermore, BiisNet achieves competitive results comparable to 32-bit full-precision IRSTD models. Remarkably, BiisNet surpasses UIU-Net by 2.76% in $mIoU$, despite using only 0.019% of its parameters and 0.080% of its computational cost. In comparison, the previously lead-

Type	Methods	Venue	Params	OPs	IRSTD-1K			NUDT-SIRST			SIRST		
					$mIoU \uparrow$	$Pd \uparrow$	$Fa \downarrow$	$mIoU \uparrow$	$Pd \uparrow$	$Fa \downarrow$	$mIoU \uparrow$	$Pd \uparrow$	$Fa \downarrow$
M	RLCM	GRSL2018	-	-	14.62	65.66	1.79	15.13	66.34	16.29	21.02	80.61	199.15
	WSLCM	GRSL2021	-	-	0.98	70.03	1502.70	0.84	74.57	5239.16	1.02	80.99	45846.16
	TLLCM	GRSL2019	-	-	5.36	63.97	0.49	7.05	62.01	4.61	11.03	79.47	7.27
	MSLCM	IPT2018	-	-	5.34	59.93	0.54	6.64	56.82	2.56	11.56	78.33	8.37
	MSPCM	IPT2018	-	-	7.33	60.27	1.52	5.85	55.86	11.59	12.83	83.27	17.77
	NRAM	RS2018	-	-	15.24	70.68	1.69	6.93	56.4	1.92	12.16	74.52	13.85
	RIPT	JSTARS2018	-	-	14.10	77.55	2.83	29.44	91.85	34.43	11.05	79.08	22.61
	PSTNN	RS2019	-	-	24.57	71.99	3.52	14.84	66.13	4.41	22.40	77.95	29.11
	MSLSTIPT	RS2023	-	-	11.43	79.03	152.40	8.34	47.39	8.81	10.30	82.13	1131.00
F	ACM	WACV2021	407	2.65	59.15	90.57	2.04	64.85	96.72	2.85	69.44	92.02	22.71
	ALCNet	TGRS2021	437	2.19	61.59	89.56	1.44	61.13	97.24	2.90	61.05	87.07	55.98
	ISNet	CVPR2022	966	250.29	61.85	90.23	3.15	81.23	97.77	0.63	70.49	95.06	67.98
	RDIAN	TGRS2023	216	29.69	59.93	87.20	3.32	82.41	98.83	1.36	70.74	95.06	48.16
	DNA-Net	TIP2022	4665	111.55	64.88	89.22	2.59	89.81	98.90	0.64	74.81	93.54	38.28
	ISTDU-Net	GRSL2022	2818	63.66	65.71	90.57	1.37	92.34	98.51	0.55	75.93	96.20	38.90
	UIU-Net	TIP2023	50540	434.93	65.69	91.25	1.34	90.51	98.83	0.83	77.53	92.39	9.33
	IRPruneDet	AAAI2024	180	-	64.54	91.74	1.60	-	-	-	75.12	98.61	2.96
	MSHNet	CVPR2024	4065	48.39	67.87	92.86	0.88	80.55	97.99	1.17	-	-	-
B	BNN	NeurIPS2016	31	0.91	6.10	51.68	36.00	17.79	54.70	14.72	21.81	78.63	30.00
	BiConnect	ECCV2015	19	0.30	32.04	53.68	8.99	29.75	71.32	21.04	30.89	61.45	9.04
	Bi-realNet	ECCV2018	19	0.70	55.76	81.41	2.89	67.08	81.41	2.89	34.73	62.98	19.54
	ReActNet	ECCV2020	20	0.70	29.76	44.25	3.74	36.08	68.14	14.61	24.80	56.11	22.97
	IRNet	CVPR2020	24	0.87	56.67	76.68	1.17	76.49	93.96	4.58	53.04	80.92	9.41
	BBCU	ICLR2023	18	0.30	52.23	81.41	3.65	58.29	79.47	6.17	53.94	78.62	5.03
	BiisNet	Ours	10	0.35	68.45	88.85	0.99	82.88	96.40	2.70	66.73	92.40	8.34

Table 2. The quantitative comparison between the proposed BiisNet and model-based (M), full-precision (F), and binary network (B) methods on the IRSTD-1K, SIRST and NUDT-SIRST datasets. *Params* (K) and *OPs* (G) represent the number of parameters and operations, respectively. The evaluation metrics are $mIoU$ (%), Pd (%), and Fa ($\times 10^{-5}$).

ing binary network, IRNet, falls 9.02% behind UIU-Net in $mIoU$. Compared to the IRPruneDet, which applies network pruning, BiisNet outperforms it by 2.76% in $mIoU$ increase, achieving 68.45% $mIoU$ compared to 65.69% $mIoU$ in IRPruneDet, while using only 0.019% of the parameters and 0.080% of the computational cost.

Statistics on the SIRST and NUDT-SIRST datasets yield similar findings. On NUDT-SIRST dataset, compared to IRNet, the second-best binary architecture, BiisNet achieves a 6.39% $mIoU$ improvement, reaching 82.88% compared to IRNet’s 76.49% while maintaining a 41.05% lower Fa rate, 58.33% fewer parameters, and 56.47% reduced computational cost. Compared to full-precision models, BiisNet also delivers highly competitive results. Specifically, compared to MSHNet, BiisNet achieves a 2.33% higher $mIoU$ while using only 0.24% of the parameters and 2.3% of the computational cost. These findings strongly suggest that BiisNet is highly promising for deployment on low-power edge devices, making it a compelling solution for efficient infrared small target detection.

4.4. Qualitative Analysis

As shown in Figure 6, we present a qualitative comparison of the proposed BiisNet against other IRSTD models. From the visualization results, it is evident that ACM and ALCNet suffer from a high number of false positives, leading to significant non-target artifacts. While DNANet demonstrates relatively high detection accuracy, it exhibits deviations in learning fine-grained target details and still produces a certain degree of false detections. UIU-Net performs relatively well in the given scenarios; however, its ability to predict target shapes and fine details remains suboptimal. In comparison, the proposed BiisNet achieves higher detection accuracy and stronger capability in learning fine-grained details, further validating its superiority in infrared small target detection tasks.

4.5. Ablation Study

To distinguish the effectiveness of the components of BiisNet, we adopt a 4-stage U-shaped binary network as the baseline model. This model follows the architecture described in Sec. 3 but does not incorporate the DB Conv and ReDistribution modules. Instead, it employs the same gra-

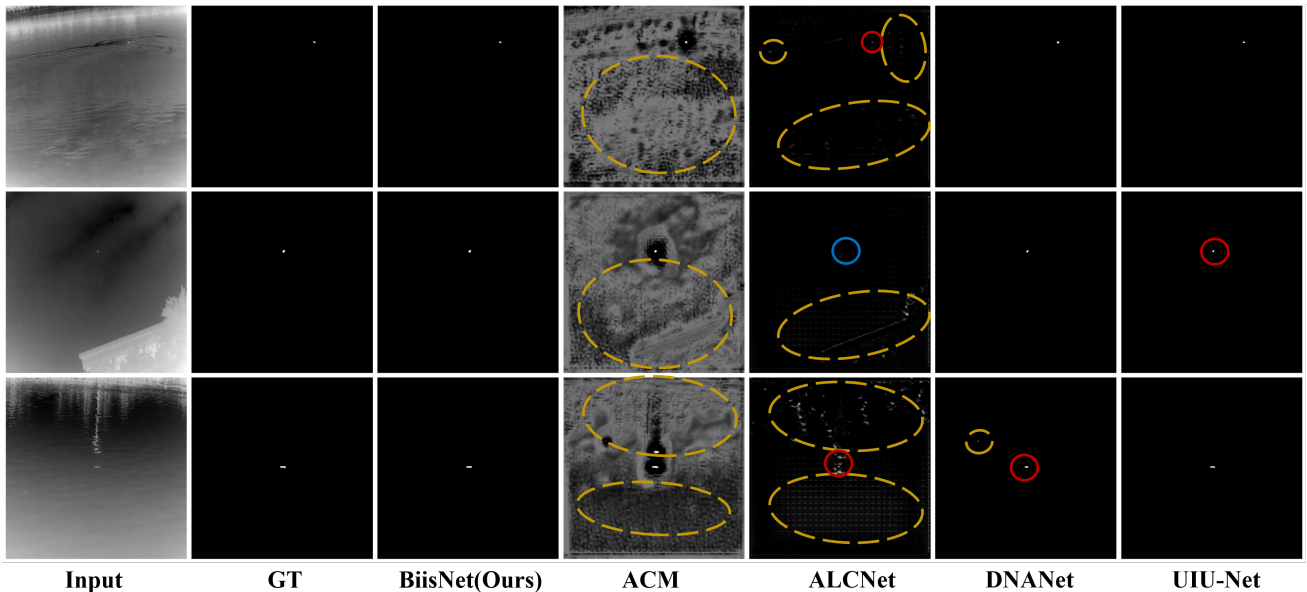


Figure 6. Visualization results of BiisNet compared with ACM [7], ALCNet [6], DNANet [18], UIUNet [39]. The red circles in the figure indicate areas where target features are learned with relatively high error, while the blue circles indicate instances where the target detection fails. The yellow circles represent false alarms.

Methods	$mIoU(\%)$	$Pd(\%)$	Params (K)	OPs (G)
4-Stages Baseline	56.93	86.86	74	0.57
+DySoftSign	61.11	84.12	74	0.57
+ReDistribution	62.74	86.48	84	0.57
Block + DB Conv	67.02	88.51	72	0.42
DS/US/FU + DB Conv	67.68	88.85	66	0.38
3-Stages BiisNet	68.45	88.85	10	0.35

Table 3. The ablation study of BiisNet.

gradient estimation method as IRNet.

As shown in Sec. 4.5, when replacing the STE with DySoftSign for gradient estimation, the model’s $mIoU$ rapidly increases to 61.11%. This indicates that a lower-error approximation of $Sign()$ allows the BNN model closer to full-precision methods. Subsequently, the Re-Distribution module adds a linear mapping term $\alpha X'_f + \beta$ within the Binary Block, enhancing its representational capacity. This modification helps reach a good trade-off between the parameter count and accuracy.

By replacing the second binary convolution layer in the Binary Block with DB Conv, the model achieves a significant $mIoU$ improvement of 4.28% while simultaneously reducing parameter count and computational cost. This demonstrates that integrating higher-precision activation values in binary infrared small target detection networks can effectively compensate for information loss and substantially enhance the model’s expressiveness. Furthermore, replacing all binary convolutions in Down-Sample

(DS), Up-Sample (US) and Fusion (FU) modules further reduces the model’s parameter count while maintaining high $mIoU$ performance.

Since small targets in the infrared imagery occupy only a small fraction of the image and their features are lost during repeated downsampling operations, deeper network architectures become less effective for feature extraction while adding unnecessary computational and parameter overhead. Therefore, we remove the final stage and further reduce the number of Binary Blocks in the third stage. Notably, this modification significantly decreases the model’s parameter count to 10K while yielding the best $mIoU$ of 68.45% and Pd of 88.85%.

5. Conclusion

In this paper, we introduced a BNN-based method for IRSTD, BiisNet, with only 10K parameters. To the best of our knowledge, this is the first BNN-based model applied to this task. To mitigate the precision loss caused by binarization, we proposed DB Conv, which preserves full-precision activations within core binary convolution operations. This enables efficient feature extraction with extremely low parameter and computational overhead. To get precise gradient during backpropagation, we introduce DySoftSign to approximate the non-differentiable Sign function, significantly reducing gradient estimation errors.

BiisNet outperforms existing binary architectures and remains competitive with SOTA full-precision models. No-

tably, it surpasses UIU-Net by 2.76% in $mIoU$ while requiring only 0.019% of the parameters and 0.080% of the computational cost. These results highlight BiisNet’s potential for IRSTD, making it a promising solution for the deployment on edge devices.

References

- [1] Yoshua Bengio, Nicholas Léonard, and Aaron Courville. Estimating or propagating gradients through stochastic neurons for conditional computation, 2013. [2](#)
- [2] Yuanhao Cai, Yuxin Zheng, Jing Lin, Xin Yuan, Yulun Zhang, and Haoqian Wang. Binarized spectral compressive imaging. In *Advances in Neural Information Processing Systems*, pages 38335–38346. Curran Associates, Inc., 2023. [3](#)
- [3] Tianxiang Chen, Qi Chu, Bin Liu, and Nenghai Yu. Fluid dynamics-inspired network for infrared small target detection. In *Proceedings of the Thirty-Second International Joint Conference on Artificial Intelligence, IJCAI-23*, pages 590–598. International Joint Conferences on Artificial Intelligence Organization, 2023. Main Track. [3](#)
- [4] Matthieu Courbariaux, Yoshua Bengio, and Jean-Pierre David. Binaryconnect: training deep neural networks with binary weights during propagations. In *Proceedings of the 29th International Conference on Neural Information Processing Systems - Volume 2*, page 3123–3131, Cambridge, MA, USA, 2015. MIT Press. [6](#)
- [5] Yimian Dai and Yiquan Wu. Reweighted infrared patch-tensor model with both nonlocal and local priors for single-frame small target detection. *IEEE Journal of Selected Topics in Applied Earth Observations and Remote Sensing*, 10(8):3752–3767, 2017. [6](#)
- [6] Yimian Dai, Yiquan Wu, Fei Zhou, and Kobus Barnard. Attentional Local Contrast Networks for Infrared Small Target Detection. *IEEE Transactions on Geoscience and Remote Sensing*, pages 1–12, 2021. [6, 8](#)
- [7] Yimian Dai, Yiquan Wu, Fei Zhou, and Kobus Barnard. Asymmetric contextual modulation for infrared small target detection. In *IEEE Winter Conference on Applications of Computer Vision, WACV 2021*, 2021. [3, 6, 8](#)
- [8] Suyog D. Deshpande, Meng Hwa Er, Ronda Venkateswarlu, and Philip Chan. Max-mean and max-median filters for detection of small targets. In *Signal and Data Processing of Small Targets 1999*, pages 74 – 83. International Society for Optics and Photonics, SPIE, 1999. [6](#)
- [9] Chenqiang Gao, Deyu Meng, Yi Yang, Yongtao Wang, Xiaofang Zhou, and Alexander G. Hauptmann. Infrared patch-image model for small target detection in a single image. *IEEE Transactions on Image Processing*, 22(12):4996–5009, 2013. [6](#)
- [10] Shangqian Gao, Zeyu Zhang, Yanfu Zhang, Feihu Huang, and Heng Huang. Structural alignment for network pruning through partial regularization. In *Proceedings of the IEEE/CVF international conference on computer vision*, pages 17402–17412, 2023. [1](#)
- [11] The Weaver Computer Engineering Research Group. The companion to the top performance list for the same set of machines. Website. <https://forums.raspberrypi.com/viewtopic.php?t=340807>. [1](#)
- [12] Jinhui Han, Kun Liang, Bo Zhou, Xinying Zhu, Jie Zhao, and Linlin Zhao. Infrared small target detection utilizing the multiscale relative local contrast measure. *IEEE Geoscience and Remote Sensing Letters*, 15(4):612–616, 2018. [6](#)
- [13] Jinhui Han, Saed Moradi, Iman Faramarzi, Chengyin Liu, Honghui Zhang, and Qian Zhao. A local contrast method for infrared small-target detection utilizing a tri-layer window. *IEEE Geoscience and Remote Sensing Letters*, 17(10):1822–1826, 2020. [6](#)
- [14] Jinhui Han, Saed Moradi, Iman Faramarzi, Honghui Zhang, Qian Zhao, Xiaojian Zhang, and Nan Li. Infrared small target detection based on the weighted strengthened local contrast measure. *IEEE Geoscience and Remote Sensing Letters*, 18(9):1670–1674, 2020. [6](#)
- [15] Jinhui Han, Saed Moradi, Iman Faramarzi, Honghui Zhang, Qian Zhao, Xiaojian Zhang, and Nan Li. Infrared small target detection based on the weighted strengthened local contrast measure. *IEEE Geoscience and Remote Sensing Letters*, 18(9):1670–1674, 2021. [6](#)
- [16] Qingyu Hou, Liuwei Zhang, Fanjiao Tan, Yuyang Xi, Hao-liang Zheng, and Na Li. Istdu-net: Infrared small-target detection u-net. *IEEE Geoscience and Remote Sensing Letters*, 19:1–5, 2022. [6](#)
- [17] Minje Kim and Paris Smaragdis. Bitwise neural networks. *ArXiv*, abs/1601.06071, 2016. [1, 3, 4, 6](#)
- [18] Boyang Li, Chao Xiao, Longguang Wang, Yingqian Wang, Zaiping Lin, Miao Li, Wei An, and Yulan Guo. Dense nested attention network for infrared small target detection. *IEEE Transactions on Image Processing*, 32:1745–1758, 2022. [6, 8](#)
- [19] Jingzhi Li, Zidong Guo, Hui Li, Seungju Han, Ji-won Baek, Min Yang, Ran Yang, and Sungjoo Suh. Rethinking feature-based knowledge distillation for face recognition. In *Proceedings of the IEEE/CVF conference on computer vision and pattern recognition*, pages 20156–20165, 2023. [1](#)
- [20] Zhikai Li, Junrui Xiao, Lianwei Yang, and Qingyi Gu. Repqvit: Scale reparameterization for post-training quantization of vision transformers. In *Proceedings of the IEEE/CVF International Conference on Computer Vision*, pages 17227–17236, 2023. [1](#)
- [21] Mingbao Lin, Rongrong Ji, Zi-Han Xu, Baochang Zhang, Fei Chao, Mingliang Xu, Chia-Wen Lin, and Ling Shao. Siman: Sign-to-magnitude network binarization. *IEEE Transactions on Pattern Analysis and Machine Intelligence*, 45:6277–6288, 2021. [3, 4](#)
- [22] Qiankun Liu, Rui Liu, Bolun Zheng, Hongkui Wang, and Ying Fu. Infrared small target detection with scale and location sensitivity. In *Proceedings of the IEEE/CVF Conference on Computer Vision and Pattern Recognition (CVPR)*, pages 17490–17499, 2024. [1, 6](#)
- [23] Zechun Liu, Baoyuan Wu, Wenhan Luo, Xin Yang, Wei Liu, and Kwang-Ting Cheng. Bi-real net: Enhancing the performance of 1-bit cnns with improved representational capability and advanced training algorithm. In *Proceedings of the European Conference on Computer Vision (ECCV)*, pages 722–737, 2018. [2, 3, 6](#)

- [24] Zechun Liu, Zhiqiang Shen, Marios Savvides, and Kwang-Ting Cheng. Reactnet: Towards precise binary neural network with generalized activation functions. In *European Conference on Computer Vision (ECCV)*, 2020. 6
- [25] LUYue. Torch flops tools. Website. https://github.com/zugexiaodui/torch_flops. 6
- [26] Qianchen Mao, Qiang Li, Bingshu Wang, Yongjun Zhang, Tao Dai, and C. L. Philip Chen. Spirdet: Toward efficient, accurate, and lightweight infrared small-target detector. *IEEE Transactions on Geoscience and Remote Sensing*, 62:1–12, 2024. 3
- [27] Saeed Moradi, Payman Moallem, and Mohamad Farzan Sabahi. A false-alarm aware methodology to develop robust and efficient multi-scale infrared small target detection algorithm. *Infrared Physics & Technology*, 89:387–397, 2018. 6
- [28] Raspberry Pi. Flop rate for pi4b models. Website. <https://forums.raspberrypi.com/viewtopic.php?t=340807>. 1
- [29] Haotong Qin, Ruihao Gong, Xianglong Liu, Mingzhu Shen, Ziran Wei, Fengwei Yu, and Jingkuan Song. Forward and backward information retention for accurate binary neural networks. In *Proceedings of the IEEE/CVF Conference on Computer Vision and Pattern Recognition*, 2020. 6
- [30] Haotong Qin, Ruihao Gong, Xianglong Liu, Mingzhu Shen, Ziran Wei, Fengwei Yu, and Jingkuan Song. Forward and backward information retention for accurate binary neural networks. In *Proceedings of the IEEE/CVF conference on computer vision and pattern recognition*, pages 2250–2259, 2020. 2, 3
- [31] Mohammad Rastegari, Vicente Ordonez, Joseph Redmon, and Ali Farhadi. Xnor-net: Imagenet classification using binary convolutional neural networks. *ArXiv*, abs/1603.05279, 2016. 2
- [32] Olaf Ronneberger, Philipp Fischer, and Thomas Brox. U-net: Convolutional networks for biomedical image segmentation. *ArXiv*, abs/1505.04597, 2015. 3
- [33] Heng Sun, Junxiang Bai, Fan Yang, and Xiangzhi Bai. Receptive-field and direction induced attention network for infrared dim small target detection with a large-scale dataset irdst. *IEEE Transactions on Geoscience and Remote Sensing*, 61:1–13, 2023. 6
- [34] Victor T. Tom, Tamar Peli, May Leung, and Joseph E. Bondaryk. Morphology-based algorithm for point target detection in infrared backgrounds. In *Signal and Data Processing of Small Targets 1993*, pages 2–11. International Society for Optics and Photonics, SPIE, 1993. 6
- [35] Kewei Wang, Shuaiyuan Du, Chengxin Liu, and Zhiguo Cao. Interior attention-aware network for infrared small target detection. *IEEE Transactions on Geoscience and Remote Sensing*, 60:1–13, 2022. 3
- [36] Peisong Wang, Xiangyu He, Gang Li, Tianli Zhao, and Jian Cheng. Sparsity-inducing binarized neural networks. In *Proceedings of the AAAI conference on artificial intelligence*, pages 12192–12199, 2020. 3, 4
- [37] Shuanglin Wu, Chao Xiao, Longguang Wang, Yingqian Wang, Jungang Yang, and Wei An. Repisd-net: Learning efficient infrared small-target detection network via structural re-parameterization. *IEEE Transactions on Geoscience and Remote Sensing*, 2023. 3
- [38] Tianhao Wu, Boyang Li, Yihang Luo, Yingqian Wang, Chao Xiao, Ting Liu, Jungang Yang, Wei An, and Yulan Guo. Mtnet: Multilevel transunet for space-based infrared tiny ship detection. *IEEE Transactions on Geoscience and Remote Sensing*, 61:1–15, 2023. 3
- [39] X. Wu, D. Hong, and J. Chanussot. Uiu-net: U-net in u-net for infrared small object detection. *IEEE Trans. Image. Process.*, 32:364–376, 2023. 1, 6, 8
- [40] Bin Xia, Yulun Zhang, Yitong Wang, Yapeng Tian, Wenming Yang, Radu Timofte, and Luc Van Gool. Basic binary convolution unit for binarized image restoration network. *International Conference on Learning Representations*, 2023. 6
- [41] Landan Zhang and Zhenming Peng. Infrared small target detection based on partial sum of the tensor nuclear norm. *Remote Sensing*, 11(4), 2019. 6
- [42] Landan Zhang, Lingbing Peng, Tianfang Zhang, Siying Cao, and Zhenming Peng. Infrared small target detection via non-convex rank approximation minimization joint $l_{2,1}$ norm. *Remote Sensing*, 10(11), 2018. 6
- [43] Mingjin Zhang, Rui Zhang, Yuxiang Yang, Haichen Bai, Jing Zhang, and Jie Guo. Isnet: Shape matters for infrared small target detection. In *2022 IEEE/CVF Conference on Computer Vision and Pattern Recognition (CVPR)*, pages 867–876, 2022. 1, 3, 6
- [44] Mingjin Zhang, Yuchun Wang, Jie Guo, Yunsong Li, Xinbo Gao, and Jing Zhang. Irsam: Advancing segment anything model for infrared small target detection. In *European Conference on Computer Vision*, pages 233–249. Springer, 2024. 3
- [45] Mingjin Zhang, Handi Yang, Jie Guo, Yunsong Li, Xinbo Gao, and Jing Zhang. Irrunedet: Efficient infrared small target detection via wavelet structure-regularized soft channel pruning. In *AAAI*, pages 7224–7232, 2024. 6
- [46] Zhaoyang Zhang, Wenqi Shao, Jinwei Gu, Xiaogang Wang, and Luo Ping. Differentiable dynamic quantization with mixed precision and adaptive resolution. *ArXiv*, abs/2106.02295, 2021. 3
- [47] Pengju Ren Zhijun Tu, Xinghao Chen and Yunhe Wang. Adabin: Improving binary neural networks with adaptive binary sets. In *European Conference on Computer Vision (ECCV)*, 2022. 3, 4